Transactions D:
Computer Science & Engineering and
Electrical Engineering
Vol. 16, No. 2, pp. 157–162

SCIENTIA IRANICA

Theory of Optimal Mixing in Directly Modulated Laser Diodes

S. Khorasani[1,*] **and B. Cabon**[2]

Abstract. *Using a simple nonlinear model based on rate equations, and by employing a harmonic balance method, we develop a theory of optimal mixing in directly modulated semiconductor laser diodes. We perform a consistent numerical solution to the mixing in laser diodes to the arbitrary accuracy and intermodulation index* (m, n)*. Through numerical computations we demonstrate that there is an optimal bias in mixing, corresponding to a relaxation frequency,* f_r*, coinciding with the subcarrier frequency,* f_1*, at which the mixing power is maximized nearly simultaneously for all intermodulation products,* f_{mn}*. In terms of increasing the signal's current amplitude, it will be shown that it would result in a monotonic increase in the optical power of all intermodulation products, as is normally expected. More generally and for the first time to the best of our knowledge, the condition for optimal mixing power is found as* $f_{mn} = kf_r = mf_1 + nf_2$*. Applications are in data transmission beyond the resonant frequency of the laser diode as needed in future communication standards.*

Keywords: *Laser diode; Mixing; Microwave photonics.*

INTRODUCTION

Recently, there has been a growing interest in the next generation of Ultra Wide Band (UWB) optical networks, which employ higher subcarrier frequencies, since future UWB systems will explore higher frequency bands, such as the millimeter wave (MMW) band [1]. This requires wide-band frequency up-conversion of the usual MB-OFDM UWB signal occupying the 3.1-10.6 GHz spectrum, which can be easily achieved by all-optical mixers and Electrical to Optical (E/O) and back O/E (Optical to Electrical) converters that compose an optical link. Optical fiber is of benefit to huge available bandwidths suitable for high capacity networks and at a very low cost, even when higher frequencies are used in modulation of the optical carrier transmitted along the optical fiber.

In nearly all communication systems, in which nonlinear phenomena in certain devices are exploited to achieve a power boost or detection, mixers play a vital role. A very simple and cost effective mixing scheme can be obtained by the inherent nonlinearity of Laser Diodes (LD); in this case, LD is used as an E/O converter and microwave mixer, simultaneously. As will be discussed, nonlinearity stems from the stimulated emission terms in the rate equations model. All optical mixing has been demonstrated by several methods [2], but the less expensive and most simple method is to use a LD directly modulated by two RF and Local Oscillator (LO) signals. Extending the available frequency band is, of course, at the expense of power, especially if mixing uses the harmonics of input signals. We have already demonstrated the feasibility of a frequency up-conversion of UWB signals using a Vertical Cavity Surface Emitting Laser (VCSEL) [3]. This paper investigates the best conditions for mixing in laser diodes for the first time, to the best of our knowledge, with possible exploration of frequency bands far beyond the oscillation frequency of LD.

Two typical setups for the experimental realization of mixing in laser diodes are shown in Figure 1. The conventional way uses an external modulator (Figure 1a), while in our proposed method, the laser diode is directly modulated (Figure 1b). In the

1. *School of Electrical Engineering, Sharif University of Technology, Tehran, P.O. Box 11155-9363, Iran.*
2. *Institut de Microélectronique, Electromagnétisme et Photonique, IMEP, MINATEC-INPG, BP257, 38016 Grenoble Cédex, France.*
*. *Corresponding author. Email: khorasani@sina.sharif.edu*

Received 19 August 2008; received in revised form 19 January 2009; accepted 16 March 2009

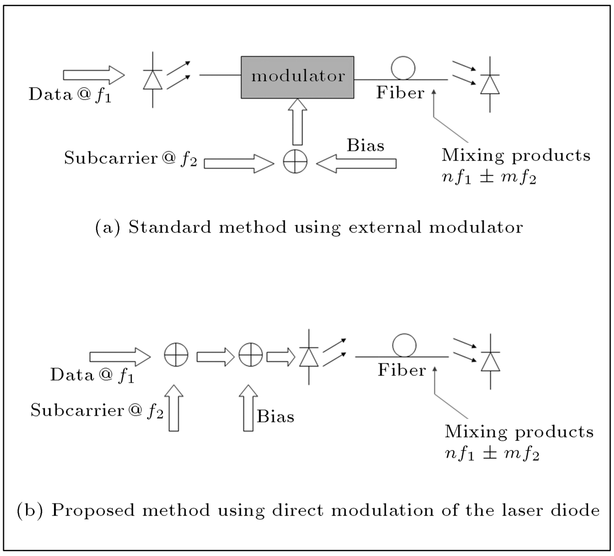

Figure 1. Illustration of mixing in laser-diode transmitters. (a) standard method using external modulator; (b) Proposed method using direct modulation of the laser diode.

theoretical formulations, we ignore the effect of mode competition, with the understanding that the diode laser under consideration is supposed to be single mode. Furthermore, the effect of gain compression which is known to be partly due to spatial hole burning has been neglected for simplicity. Whereas this phenomenon plays an important role in VCSELs [4], it is usually negligible for in-plane lasers. We also disregard the effect of thermal variations in cavity, which can be justified if the typical time-scale of electrical excitations is shorter than 1 μs [4,5].

THEORY

Here, we show that optimum mixing for a given mixing product is obtained when its frequency simply matches to the relaxation frequency of the diode. Starting directly from the rate equations with linearized gain and neglecting the spontaneous emission, gain compression and chirp, we have [6-8]:

$$\frac{dN}{dt} = \eta_i \frac{I}{qV} - \frac{N}{\tau_e} - v_g a(N - N_{tr})S, \tag{1a}$$

$$\frac{dS}{dt} = \Gamma v_g a(N - N_{tr})S - \frac{S}{\tau_p}, \tag{1b}$$

where N and S are, respectively, the spatially-averaged carrier and photon density, η_i is the carrier injection efficiency, q is electronic charge, and V is the active cavity volume. Furthermore, τ_e and τ_p are, respectively, electron and photon lifetimes, v_g is the group velocity of light, a is the linear gain coefficient, N_{tr} is the transparency carrier density and Γ is the confinement factor.

The LD is directly modulated by a two tone signal, composed of a RF subcarrier and a Local Oscillator (LO) at different angular frequencies, ω_1 and ω_2, respectively. Therefore, in the following, we suppose that the driving current of LD is composed of two sinusoids biased at some DC level I_0, such that $I(t) = I_0 + I_1 \exp(j\omega_1 t) + I_2 \exp(j\omega_2 t)$, in which I_1 and I_2 are the corresponding current amplitudes. The nonlinearity arises from NS product terms on the right-hand-side of Equation 1, so that the total carrier and photon densities may be expanded as: $N(t) = \sum N_{mn} \exp[j(m\omega_1 + n\omega_2)t]$ and $S(t) = \sum S_{mn} \exp[j(m\omega_1 + n\omega_2)t]$. Here, N_{mn} and S_{mn} correspond to the amplitudes of the intermodulation product's frequency, $\omega_{mn} = m\omega_1 + n\omega_2$, in the total carrier and photon densities, respectively. After some rearrangement we get:

$$\begin{pmatrix} j\omega_{mn} + \frac{1}{\tau_e} & -v_g a N_{tr} \\ 0 & j\omega_{mn} + \frac{1}{\tau_p} + \Gamma v_g a N_{tr} \end{pmatrix} \begin{pmatrix} N_{mn} \\ S_{mn} \end{pmatrix}$$

$$= \frac{\eta_i}{qV} \begin{pmatrix} I_{mn} \\ 0 \end{pmatrix} + v_g a \begin{pmatrix} -U_{mn} \\ \Gamma U_{mn} \end{pmatrix}, \tag{2}$$

where $I_{mn} = I_0 \delta_{m,0} \delta_{n,0} + I_1 \delta_{m,1} \delta_{n,0} + I_2 \delta_{m,0} \delta_{n,1}$ in which δ_{mn} is the Kronecker's delta, and nonlinear term U_{mn} is given by $U_{mn} = \sum S_{m-p,n-q} N_{p,q} = \sum S_{pq} N_{m-p,n-q}$. We take out the linear terms in N_{mn} and S_{mn} on the right hand side of Equation 2 to get:

$$\begin{pmatrix} j\omega_{mn} + \frac{1}{\tau_e} + v_g a S_{00} & v_g a(N_{00} - N_{tr}) \\ -\Gamma v_g a S_{00} & j\omega_{mn} + \frac{1}{\tau_p} - \Gamma v_g a(N_{00} - N_{tr}) \end{pmatrix}$$

$$\begin{pmatrix} N_{mn} \\ S_{mn} \end{pmatrix} = \frac{\eta_i}{qV} \begin{pmatrix} I_{mn} \\ 0 \end{pmatrix} + v_g a \begin{pmatrix} -V_{mn} \\ \Gamma V_{mn} \end{pmatrix}. \tag{3}$$

Here, V_{mn} retains the nonlinear terms in N_{mn} and S_{mn}, which, as long as m and n are not simultaneously zero, may be expressed as $V_{mn} = U_{mn} - S_{mn} N_{00} - S_{00} N_{mn}$. Clearly, N_{00} and S_{00} represent DC values which can be found by setting $m = n = 0$ in Equation 4, and making the rough approximation, $U_{00} = S_{00} N_{00}$. This would result in the nonlinear system of equations:

$$\begin{pmatrix} \frac{1}{\tau_e} & v_g a(N_{00} - N_{tr}) \\ 0 & \frac{1}{\tau_p} - \Gamma v_g a(N_{00} - N_{tr}) \end{pmatrix} \begin{pmatrix} N_{00} \\ S_{00} \end{pmatrix} = \frac{\eta_i}{qV} \begin{pmatrix} I_0 \\ 0 \end{pmatrix}, \tag{4}$$

which can be readily solved to obtain the well-known expressions $N_{00} = N_{tr} + \frac{1}{\Gamma \tau_p v_g a}$, and $S_{00} = \Gamma \tau_p \frac{\eta_i}{qV}(I - I_{th})$. Here, the threshold current density is given by $I_{th} = qVN_{00}/\eta_i \tau_e$.

Now, N_{mn} and S_{mn} are inversely proportional to the determinant $\Delta(\omega_{mn})$ of the 2×2 matrix of coefficients at the left-hand-side of Equation 3, in which $\Delta(\omega_{mn}) = \omega_r^2 - \omega_{mn}^2 + j\gamma\omega_{mn}$, with $\omega_r^2 = \frac{1}{\tau_e\tau_p} + v_g a\left[\frac{S_{00}}{\tau_p} - \frac{\Gamma}{\tau_e}(N_{00} - N_{tr})\right]$ and $\gamma = \frac{1}{\tau_e} + \frac{1}{\tau_p} + v_g a[S_{00} - \Gamma(N_{00} - N_{tr})]$. Clearly, ω_r is the relaxation frequency given as $\omega_r^2 = v_g S_{00}\frac{a}{\tau_p} = \Gamma\eta_i v_g \frac{a}{qV}(I - I_{th})$.

If $\gamma < \omega_r$, which is the usual case at bias currents well above the threshold, then $|\Delta(\omega)|$ reaches a minimum at $\omega = \omega_p = (\omega_r^2 - \frac{1}{2}\gamma^2)^{\frac{1}{2}}$. This shows that, as a crude approximation, a peak of photon and carrier density at the harmonic, ω_{mn}, appears when $m\omega_1 + n\omega_2 = \omega_p \approx \omega_r$. This completes our assertion. Finally, by selecting $\omega = \omega_1 = \omega_2$, it can be easily seen that this conclusion is also in agreement with the previous results on the harmonic content of a single-frequency modulated laser diode where maxima in the harmonic powers are expected to occur at $\omega = \omega_r/n$ [6,7].

NUMERICAL RESULTS

Frequency Domain Simulation

Solutions of Equation 3 are obtained by an iterative scheme. To increase the speed of convergence, we employ a perturbation method. For every scanning parameter, the known set of N_{mn} and S_{mn} obtained in the last step are used as initial values to start the next point. This enabled us to reduce the computation time significantly and also to improve convergence. Numerical values of parameters are given in Table 1. Hence, we get $I_{th} = 3.1$ mA.

Figures 2 and 3 display a variation of optical output mixing power in dBm at frequency f_{mn}, as a function of bias current, I_b, of the LD, while input frequency, f_1, is fixed. This way, by varying I_b, the relaxation frequency, f_r, is varied as well. For both cases current amplitudes are equal and set to 0.1 mA.

Figure 2 clearly shows that optimum mixing power is achieved near the relaxation frequency. In this example $f_1 = 11.6$ GHz and $f_2 = f_1/10 = 1.16$ GHz. As is evident, all intermodulation products reach a maximum when the bias current is selected in such a way that the corresponding relaxation frequency matches the subcarrier at f_1, the corresponding value of I_b is, here, 7 mA. There is a slight shift in the maxima of intermodulation product powers when $n \neq 0$, with respect to the dashed line that represents the bias current coinciding with a relaxation frequency of $f_r = f_1$. This displacement towards higher frequencies can be attributed to the fact that one would expect the peaks to occur when $f_{mn} = f_r = mf_1 + nf_2$ roughly holds in agreement with the theory. Through the same

Table 1. Numerical values of laser diode parameters.

Parameter	Description	Value
η_i	Injection efficiency	100%
V	Cavity volume	1.4 μm^3
N_{tr}	Transparency carrier density	7.5×10^{16} cm^{-3}
a	Differential gain	1.33×10^{-16} cm^2
Γ	Confinement factor	0.15
v_g	Group velocity	10^{10} cm/s
τ_e	Carrier lifetime	100 ps
τ_p	Photon lifetime	3.8 ps

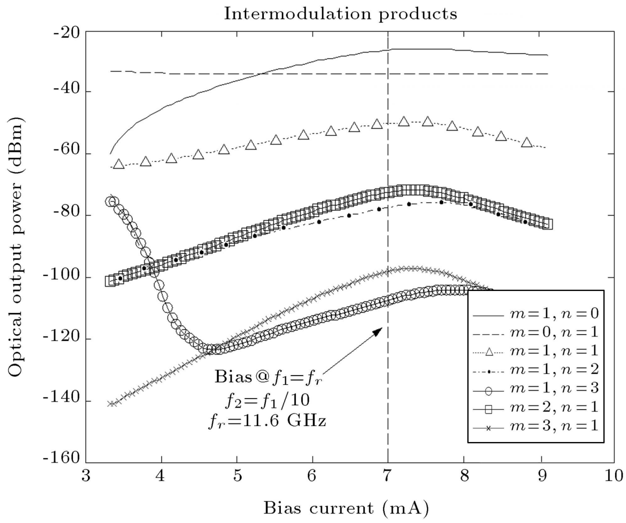

Figure 2. Variation of output optical power corresponding to the intermodulation products versus bias current ($f_2 = f_1/10$; $f_2 = 11.6$ GHz).

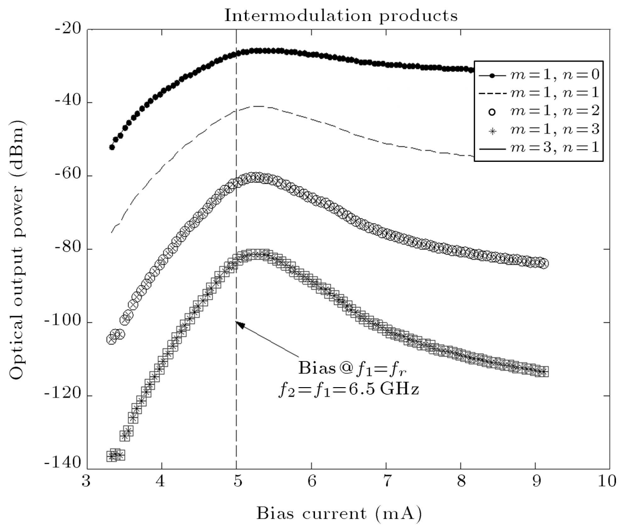

Figure 3. Variation of output optical power corresponding to the intermodulation products versus bias current ($f_1 = f_2 = 6.5$ GHz).

method for the input frequencies of $f_1 = 6.5$ GHz and $f_2 = f_1/10 = 0.65$ GHz, we find that the optimum bias is reached at $I_b = 5$ mA, giving $f_r = 6.5$ GHz, coinciding again with $f_r = f_1$.

In Figure 3, $f_2 = f_1 = 6.5$ GHz are selected. Again, there is an optimal bias current around 5 mA corresponding to a relaxation frequency of 6.5 GHz and maximizing mixing power. Therefore, as a rule of thumb in mixing, we can conclude that there exists an optimal bias current corresponding to a relaxation frequency equal to the subcarrier frequency, at which the maximum mixing can be attained. Since both frequencies are chosen to be the same, curves corresponding to the pairs of (m, n) and (n, m) coincide when $m \neq n$.

In both Figures 2 and 3, it may be noticed that the intermodulation product maxima happen at a slightly higher bias current, deviated from the theoretical optima. This can be understood in the weakly nonlinear regime if we observe that the maxima happen roughly at the zeros of the derivative of the following expression:

$$\frac{\partial}{\partial \omega_1} \prod_{mn} |\Delta(\omega_{mn})| = \frac{\partial}{\partial \omega_1} \left| \prod_{mn} \Delta(m\omega_1 + n\omega_2) \right| = 0, \tag{5}$$

which represent the denominator of the total transfer function. The general solution to the above equation is obviously very complicated, but it can be greatly simplified by investigating the particular case of $\omega = \omega_1 = \omega_2$, and noting that zeros of Equation 5 almost coincide with the roots of:

$$\mathrm{Re}\left\{ \prod_{mn} \Delta[(m+n)\omega] \right\} = 0, \tag{6}$$

due to the fact that $\gamma^2 << \omega_r^2$ (for the diode concerned at $I_b = 7$ mA, we have $\gamma^2 \sim 0.15\ \omega_r^2$). Then, ignoring all intermodulation products of order three and the above results in:

$$\mathrm{Re}\left\{ \Delta(\omega)^2 \Delta(2\omega) \right\} \sim 0. \tag{7}$$

The approximate roots of this equation, correct to the second order in γ, and close to the resonant frequency (obtained by Mathematica) are given by $\omega \sim \omega_r + \frac{1}{2}\gamma(\gamma/\omega_r \pm 1)$. For the considered laser diode at the bias current of 7 mA, this gives a 20% difference with regard to the relaxation frequency; this is while a full numerical solution incorporating a higher number of harmonics predicts an 8.5% difference for dominant poles. In Figures 2 and 3, one could observe, respectively, a 6% and 7% deviation from the bias current corresponding to the relaxation resonant frequency. This could at least partially show that one could expect the maxima to happen at a different, but close, bias current corresponding to the relaxation resonant frequency. In practice, it has been found that up-conversion slightly beyond the relaxation frequency is possible [3].

Consequently, an extension of the condition for maximum mixing power is found as:

$$f_{mn} = kf_r = mf_1 + nf_2, \tag{8}$$

where again f_{mn} is the mixing frequency at which the maximum mixing power is obtained and k, m, and n are integers. Of course at the expense of power, higher harmonic mixing is obtained and the mixing frequency, f_{mn}, is shifted far beyond the resonance frequency, f_r, of the LD. For example, in Figure 3, $m = n = 1$ gives a mixing frequency at 13 GHz twice the f_r value ($k = 2$, $m = n = 1$), while $(k, m, n) = (4, 1, 3)$ gives a mixing frequency of 26 GHz with a mixing power 20 dB lower, under the same optimum bias conditions.

In Figure 4, we investigate the effect of variations of the current amplitude. The frequency and amplitude of the RF subcarrier are fixed, respectively, at $f_1 = f_r = 9.34$ GHz and 3 mA. The frequency of the LO signal is also kept fixed at $f_2 = f_1/10 = 0.934$ GHz, but its amplitude is varied between 10 μA and 1 mA. As normally expected, the trend is a monotonic increase in the power of all intermodulation products versus the current amplitude of the LO signal.

When Figure 4 is redrawn with the current amplitude on the horizontal axis in dBm given by $I(dBm) = 20\log_{10}\ (I/1\ \text{mA})$ as illustrated in the inset in Figure 4, then one could recover the standard slopes for the second-, third- and fourth-order intermodulation products, respectively, as 1.05 dB/dB, 2.12 dB/dB and 3.18 dB/dB. Here, no saturation in the harmonic powers could be expected due to the

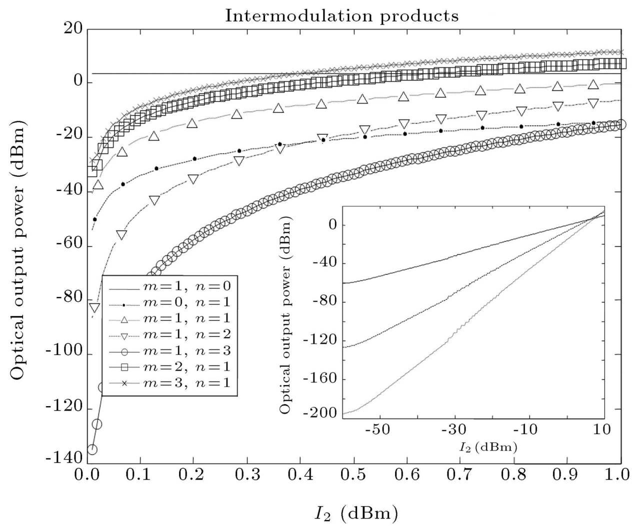

Figure 4. Optical output power of intermodulation products versus signal amplitude at fixed frequency. The inset shows the intermodulation products versus input current amplitude on the logarithmic scale.

over-simplified model, which exploits linear gain with no gain compression. This also partially justifies the validity of the harmonic balance model.

Time-Domain Simulation

In order to observe the behavior of the system, one may alternatively integrate the governing equations in the time-domain and perform a Fourier transform to observe the output. We have done this for the input current:

$$I(t) = I_b + I_1 \cos(2\pi f_1 t) + I_2 \cos(2\pi f_2 t), \tag{9}$$

with $I_b = 7$ mA, $I_1 = I_2 = 3$ mA, $f_1 = 2.5$ GHz and $f_2 = 3.53$ GHz. The input current to the diode which consists of two frequencies, biased at 7 mA, is shown in Figure 5. The simulated carrier density response in the cavity of the laser diode is shown in Figure 6 over the first 10 nsec time span of the output. There is a delay in the average carrier density, which is clearly associated with the step response to the input DC bias. In Figure 7, the optical output power from the laser diode under mixing has been shown. Photodiodes have a greater linear response over a relatively wide frequency range, and it can be assumed that the amplitude of the detected current at the receiver is proportional to the optical output power. After integration for 1000 cycles and doing a fast-Fourier transform, the spectrum of the detected output power is obtained, which clearly shows the peaks corresponding to the mixing products, as shown in Figure 8.

Clearly, if the input signal at f_1 is not single-frequency, then the peaks would broaden. The available bandwidth of mixing would be, therefore, strongly dependent on the choice of the mixing product of interest and the distance to the neighboring dominant

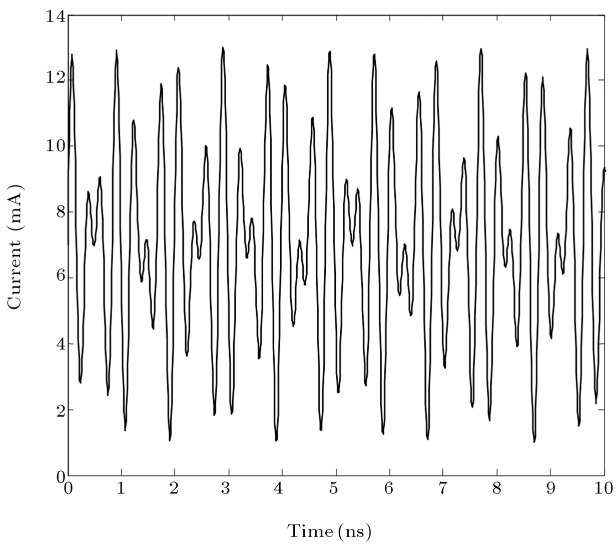

Figure 5. Two-frequency input current to the laser diode.

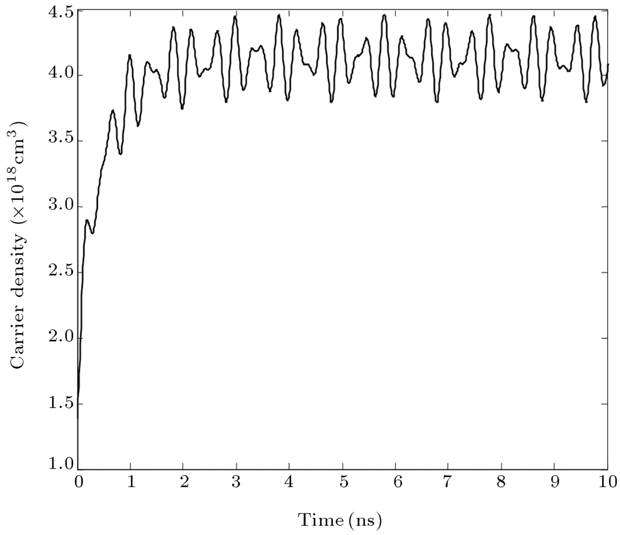

Figure 6. Simulated carrier density response in the cavity of the laser diode.

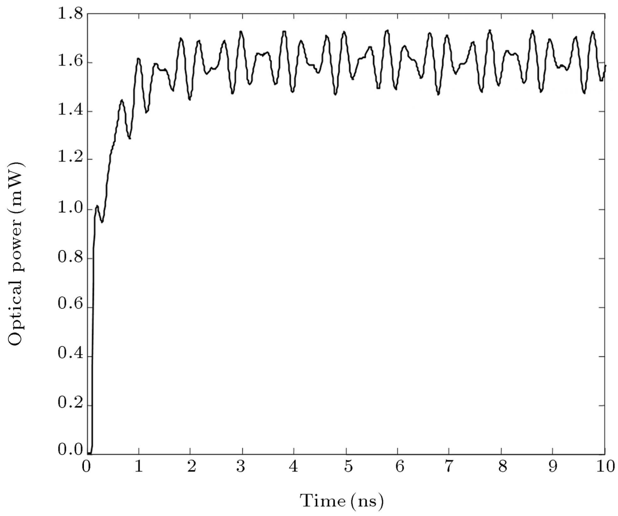

Figure 7. Simulated optical output power from the laser diode under mixing.

mixing products. For instance, if $(m, n) = (1, 1)$ is chosen as the desired intermodulation product, then the available bandwidth would be simply given by $\Delta f = \frac{1}{2}|f_1 - f_2|$. Clearly, this limitation is even dependent on the strength of signals. For instance, if we choose identical carrier and signal frequencies, $f_1 = f_2$, then all intermodulation products with $n + m = 2$ would coincide with $(m, n) = (1, 1)$. For comparable amplitudes of the signal and carrier, this would normally result in a significant crossover among products and, therefore, loss of data. However, typically the signal amplitude is much weaker than the subcarrier frequency, and the effect of overlapping intermodulations of a higher order could be neglected. The available bandwidth in that case would be, practically, $\Delta f = \frac{1}{2} f_1$.

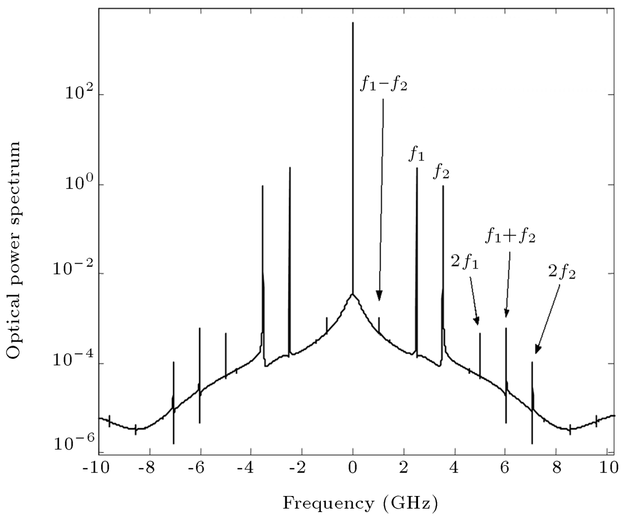

Figure 8. Spectrum of output power detected via a photo-diode.

CONCLUSION

We developed a nonlinear harmonic balance method to describe the mixing in directly modulated laser diodes. We have shown the existence of an optimal operation point through theory and numerical simulations. Frequency- and time-domain numerical tests for the nonlinear model were in reasonable agreement with theoretical predictions. This enables one to achieve maximum mixing power through a proper choice of diode and/or operating parameters. This can be exploited in future UWB standards where there is a need for converting UWB in a 60 GHz range and where very low cost optical solutions, based on innovative microwave-photonics concepts, can address the challenges of low-cost Wireless-Personal Area Networks (WPANs).

REFERENCES

1. Laskar, J., Pinel, S., Dawn, D., Sarkar, S., Perumana, B. and Sen, P. "The next wireless wave is a millimeter wave", *Microwave Journal*, **50**(8), p. 22 (2007).
2. Maury, G., Hilt, A., Berceli, T., Cabon, B. and Vilcot, A. "Microwave frequency conversion methods by optical interferometer and photodiode", *Special Issue on Microwave and Millimeter-Wave Photonics II, IEEE Trans. Microwave Th. Tech.*, **MTT-45**(8), pp. 1481-1485 (1997).
3. Schimpf, A., Bucci, D. and Cabon, B. "Low cost optical up-conversion of IR-UWB signals beyond the relaxation frequency of a vertical cavity surface emitting laser (VCSEL)", *Proc. 2008 IEEE Int. Conf. Ultra-Wideband (ICUWB2008)*, Hannover, Germany, **2**, pp. 25-28 (Sept. 10-12, 2008).
4. Gustavsson, J.S., Vukusic, J.A., Bengtsson, J. and Larsson, A. "A comprehensive model for the modal dynamics of vertical-cavity surface-emitting lasers", *IEEE J. Quantum Electron.*, **38**(2), pp. 203-212 (2002).
5. Gustavsson, J.S., Haglund, A., Bengtsson, J. and Larsson, A. "High-speed digital modulation characteristics of oxide-confined vertical-cavity surface-emitting lasers-numerical simulations consistent with experimental results", *IEEE J. Quantum Electron.*, **38**(8), pp. 1089-1096 (2002).
6. Zandi, H., Bavafa, M., Chamanzar, M. and Khorasani, S. "Analysis of power harmonic content and relaxation resonant frequency of a diode laser", *Proc. SPIE*, **6468**, 6468J (2007); Bavafa, M., Zandi, H., Chamanzar, M. and Khorasani, S. "Optimal operation point for the primary harmonic content of a modulated laser diode", *Proc. 6th WSEAS Int. Conf. Microelectronics, Nanoelectronics, Optoelectronics*, pp. 86-91, Istanbul (2007).
7. Zandi, H., Bavafa, M., Chamanzar, M. and Khorasani, S. "Harmonic content and relaxation resonant frequency of a modulated laser diode", *Scientia Iranica, Transactions D*, **16**(2), pp. 145-156 (2009).
8. Coldren, L.A. and Corzine, S.W., *Diode Lasers and Photonic Integrated Circuits*, John Wiley & Sons (1995).